

# Effect of pH and Reaction Time on the Structures of Early Lanthanide(III) Borate Perchlorates

Matthew J. Polinski,<sup>†</sup> Shuao Wang,<sup>†</sup> Evgeny V. Alekseev,<sup>‡,§</sup> Justin N. Cross,<sup>†</sup> Wulf Depmeier,<sup>||</sup> and Thomas E. Albrecht-Schmitt<sup>\*,†</sup>

<sup>†</sup>Department of Chemistry and Biochemistry, Florida State University, Tallahassee, Florida 32306, United States

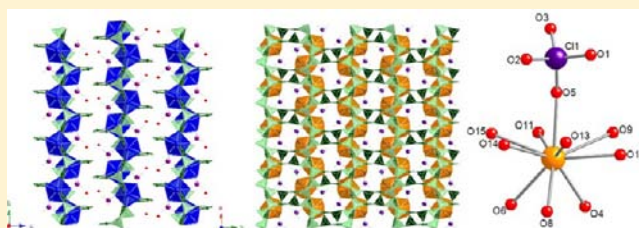
<sup>‡</sup>Forschungszentrum Jülich GmbH, Institute for Energy and Climate Research (IEK-6), 52428 Jülich, Germany

<sup>§</sup>Institut für Kristallographie, RWTH Aachen University, D-52066 Aachen, Germany

<sup>||</sup>Institut für Geowissenschaften, Universität zu Kiel, 24118 Kiel, Germany

## S Supporting Information

**ABSTRACT:** Reactions of  $\text{LnCl}_3 \cdot 6\text{H}_2\text{O}$  ( $\text{Ln} = \text{La-Nd, Sm, Eu}$ ), concentrated (11 M) perchloric acid, and molten boric acid result in the formation of four different compounds. These compounds are  $\text{Ln}[\text{B}_8\text{O}_{10}(\text{OH})_6(\text{H}_2\text{O})\text{-(ClO}_4\text{)}] \cdot 0.5\text{H}_2\text{O}$  ( $\text{Ln} = \text{La-Nd, Sm}$ ),  $\text{Pr}[\text{B}_8\text{O}_{11}(\text{OH})_4(\text{H}_2\text{O})\text{-(ClO}_4\text{)}]$ ,  $\text{Ln}[\text{B}_7\text{O}_{11}(\text{OH})(\text{H}_2\text{O})_2(\text{ClO}_4)]$  ( $\text{Ln} = \text{Pr, Nd, Sm, and Eu}$ ), and  $\text{Ce}[\text{B}_8\text{O}_{11}(\text{OH})_4(\text{H}_2\text{O})(\text{ClO}_4)]$ . All Ln(III) cations are ten-coordinate with a capped triangular cupola geometry and contain an inner-sphere, monodentate perchlorate moiety. This geometry is obtained because of the coordination of the oxygen donors within the polyborate sheet which create triangular holes and provide residence for the lanthanide metal centers. Aside from  $\text{Ln}[\text{B}_8\text{O}_{10}(\text{OH})_6(\text{H}_2\text{O})\text{-(ClO}_4\text{)}] \cdot 0.5\text{H}_2\text{O}$  ( $\text{Ln} = \text{La-Nd, Sm}$ ), which are two-dimensional sheet structures, all other compounds are three-dimensional frameworks in which the layers are tethered together by  $\text{BO}_3$  units found roughly perpendicular to the sheets. Furthermore, a change in product is observed depending on the reaction duration while holding all other synthetic variables constant. This report also demonstrates that lanthanide borates can be prepared in extreme acidic conditions.



## ■ INTRODUCTION

The perchlorate anion is considered an outer-sphere ligand when reacted with soft metal ions but can be either inner- or outer-sphere when reacted with hard ions. Under the Pearson definition, trivalent lanthanides and actinides are considered hard ions.<sup>1</sup> For many years it was thought that, because of the large hydration energies,<sup>2</sup> solid lanthanide perchlorates could not be obtained from aqueous solutions.<sup>3</sup> The perchlorate anion was also expected to be noncoordinating in acidic media.<sup>4,5</sup> Nevertheless, within the past 20 years, examples of hydrated and anhydrous lanthanide and actinide perchlorates from aqueous media obtained under mild hydrothermal or slow evaporation methods and over a wide range of pH values have surfaced. These studies have shown that perchlorate in aqueous solution can be an inner-sphere ligand with both bridging and multidentate binding modes.<sup>6–9</sup> Additionally, when organics, such as hexamethylphosphorotriamide (HMPA),<sup>10</sup> urea,<sup>11</sup> and formate<sup>12</sup> were used in conjunction with the lanthanides and actinides, perchlorate anion was found to be an outer-sphere ligand, as it was easily outcompeted by the other ligands. It should be noted that the experimental conditions used to obtain the above compounds were either mild hydrothermal conditions<sup>7,10</sup> or slow/vacuum assisted evaporations.<sup>6,8,9,11,12</sup> Conversely, when oxalate was present in the reaction vessel, perchlorate was found to reside in the first coordination sphere,

was both mono- and bidentate, and was obtained under hydrothermal conditions in relatively acidic ( $\text{pH} = 3$ ) conditions.<sup>7</sup>

The above examples are not meant to be fully exhaustive of all studies of lanthanides that contain perchlorate both as an inner- or outer-sphere ligand but meant to highlight the variability of perchlorate when used in conjunction with trivalent lanthanides and/or actinides under relatively similar conditions. In fact, a number of other factors may contribute to the inner/outer-sphere nature of perchlorate in those systems that include, but are not limited to, the role and/or identity of the organic ligand present, solution conditions (i.e., pH, ionic strength, etc.), and activity of perchlorate in the respective reaction. As similar synthetic preparations have been used to prepare lanthanide compounds with both inner- and outer-sphere perchlorate, these other factors must, in fact, play a role.

Borate can form structurally diverse polymeric networks as both  $\text{BO}_3$  and  $\text{BO}_4$  units can combine in a vast number of ways to form clusters, chains, sheets, or frameworks.<sup>13–15</sup> Additionally, the borate network is sensitive to experimental conditions such as temperature, counterions, stoichiometry, and pH. Molten boric acid as a reactive flux media has been used as a

Received: July 2, 2012

Published: October 9, 2012

**Table 1. Crystallographic Data for La[B<sub>8</sub>O<sub>10</sub>(OH)<sub>6</sub>(H<sub>2</sub>O)(ClO<sub>4</sub>)]·0.5H<sub>2</sub>O (LaBClO-1), Ce[B<sub>8</sub>O<sub>10</sub>(OH)<sub>6</sub>(H<sub>2</sub>O)(ClO<sub>4</sub>)]·0.5H<sub>2</sub>O (CeBClO-1), Pr[B<sub>8</sub>O<sub>10</sub>(OH)<sub>6</sub>(H<sub>2</sub>O)(ClO<sub>4</sub>)]·0.5H<sub>2</sub>O (PrBClO-1), Nd[B<sub>8</sub>O<sub>10</sub>(OH)<sub>6</sub>(H<sub>2</sub>O)(ClO<sub>4</sub>)]·0.5H<sub>2</sub>O (NdBClO-1), and Sm[B<sub>8</sub>O<sub>10</sub>(OH)<sub>6</sub>(H<sub>2</sub>O)(ClO<sub>4</sub>)]·0.5H<sub>2</sub>O (SmBClO-1)**

	LaBClO-1	CeBClO-1	PrBClO-1	NdBClO-1	SmBClO-1
mass	604.84	606.05	606.84	610.17	616.28
color and habit	colorless, tablet	colorless, tablet	colorless, tablet	colorless, tablet	colorless, tablet
space group	<i>P</i> <sub>2</sub> <sub>1</sub> / <i>n</i>	<i>P</i> <sub>2</sub> <sub>1</sub> / <i>n</i>	<i>P</i> <sub>2</sub> <sub>1</sub> / <i>n</i>	<i>P</i> <sub>2</sub> <sub>1</sub> / <i>n</i>	<i>P</i> <sub>2</sub> <sub>1</sub> / <i>n</i>
<i>a</i> (Å)	9.858(8)	9.8399(15)	9.8135(6)	9.796(8)	9.791(3)
<i>b</i> (Å)	8.243(6)	8.2154(13)	8.2067(6)	8.200(7)	8.205(2)
<i>c</i> (Å)	21.418(16)	21.378(3)	21.3178(14)	21.248(18)	21.227(6)
$\beta$ (deg)	96.994(9)	97.024(2)	97.102(5)	97.171(11)	97.216(3)
<i>V</i> (Å <sup>3</sup> )	1727.0(2)	1715.2(5)	1703.7(2)	1693.0(2)	1691.8(8)
<i>Z</i>	4	4	4	4	4
<i>T</i> (K)	100(2)	100(2)	100(2)	100(2)	100(2)
$\lambda$ (Å)	0.71073	0.71073	0.71073	0.71073	0.71073
maximum $2\theta$ (deg)	27.64	27.66	28.22	27.53	28.34
$\rho$ calcd (g cm <sup>-3</sup> )	2.326	2.347	2.366	2.393	2.420
$\mu$ (Mo <i>K</i> $\alpha$ )	27.39	29.22	31.30	33.38	37.43
<i>R</i> ( <i>F</i> ) for $F_o^2 > 2\sigma(F_o^2)^a$	0.0388	0.0293	0.0529	0.0390	0.0445
<i>R</i> <sub>w</sub> ( $F_o^2$ ) <sup>b</sup>	0.0898	0.0732	0.1117	0.0886	0.1006

$$^a R(F) = \frac{\sum \|F_o\| - |F_c|}{\sum |F_o|}, \quad ^b R(F_o^2) = \left[ \frac{\sum w \|F_o^2\| - |F_c^2|}{\sum w (F_o^2)} \right]^{1/2}.$$

**Table 2. Crystallographic Data for Ce[B<sub>8</sub>O<sub>11</sub>(OH)<sub>4</sub>(H<sub>2</sub>O)(ClO<sub>4</sub>)] (CeBClO-2), Pr[B<sub>8</sub>O<sub>11</sub>(OH)<sub>4</sub>(H<sub>2</sub>O)(ClO<sub>4</sub>)] (PrBClO-2), Pr[B<sub>7</sub>O<sub>11</sub>(OH)(H<sub>2</sub>O)<sub>2</sub>(ClO<sub>4</sub>)] (PrBClO-3), Nd[B<sub>7</sub>O<sub>11</sub>(OH)(H<sub>2</sub>O)<sub>2</sub>(ClO<sub>4</sub>)] (NdBClO-2), Sm[B<sub>7</sub>O<sub>11</sub>(OH)(H<sub>2</sub>O)<sub>2</sub>(ClO<sub>4</sub>)] (SmBClO-2), and Eu[B<sub>7</sub>O<sub>11</sub>(OH)(H<sub>2</sub>O)<sub>2</sub>(ClO<sub>4</sub>)] (EuBClO-1)**

	CeBClO-2	PrBClO-2	PrBClO-3	NdBClO-2	SmBClO-2	EuBClO-1
mass	582.05	582.84	540.03	543.36	549.47	551.08
color and habit	colorless, tablet	colorless, tablet	colorless, tablet	colorless, tablet	colorless, tablet	colorless, tablet
space group	<i>P</i> <sub>2</sub> <sub>1</sub> / <i>n</i>	<i>P</i> <sub>2</sub> <sub>1</sub> / <i>c</i>	<i>P</i> <sub>2</sub> <sub>1</sub> / <i>n</i>	<i>P</i> <sub>2</sub> <sub>1</sub> / <i>n</i>	<i>P</i> <sub>2</sub> <sub>1</sub> / <i>n</i>	<i>P</i> <sub>2</sub> <sub>1</sub> / <i>n</i>
<i>a</i> (Å)	8.212(7)	9.814(9)	8.1495(19)	8.1236(8)	8.099(2)	8.075(7)
<i>b</i> (Å)	18.937(15)	8.190(7)	17.070(4)	17.0348(17)	17.009(4)	16.941(15)
<i>c</i> (Å)	9.848(8)	19.158(16)	9.805(2)	9.7954(10)	9.771(3)	9.744(9)
$\beta$ (deg)	90	102.366(19)	90.507(3)	90.4960(10)	90.561(3)	90.516(12)
<i>V</i> (Å <sup>3</sup> )	1531(2)	1504(2)	1363.9(5)	1355.5(2)	1345.8(6)	1333(2)
<i>Z</i>	4	4	4	4	4	4
<i>T</i> (K)	100(2)	100(2)	100(2)	100(2)	100(2)	100(2)
$\lambda$ (Å)	0.71073	0.71073	0.71073	0.71073	0.71073	0.71073
maximum $2\theta$ (deg.)	27.59	27.82	28.28	27.58	27.65	27.69
$\rho$ calcd (g cm <sup>-3</sup> )	2.524	2.574	2.630	2.663	2.712	2.746
$\mu$ (Mo <i>K</i> $\alpha$ )	32.60	35.32	38.74	41.34	46.69	50.14
<i>R</i> ( <i>F</i> ) for $F_o^2 > 2\sigma(F_o^2)^a$	0.0549	0.0591	0.0539	0.0413	0.0294	0.0402
<i>R</i> <sub>w</sub> ( $F_o^2$ ) <sup>b</sup>	0.1109	0.1426	0.1474	0.0966	0.0609	0.0826

$$^a R(F) = \frac{\sum \|F_o\| - |F_c|}{\sum |F_o|}, \quad ^b R(F_o^2) = \left[ \frac{\sum w \|F_o^2\| - |F_c^2|}{\sum w (F_o^2)} \right]^{1/2}.$$

facile method for producing lanthanide and actinide borates.<sup>16–18</sup> We have recently reported the complete lanthanide and actinide(III) (Pu–Cm) borate series that form when chloride is present in the reactions<sup>17</sup> as well as the early lanthanide (La–Nd) borate series when both bromide and iodide are present.<sup>18</sup> These studies demonstrated that the borate network coordinates to the metal center in such a manner to force unusual geometries as well as the effect that the capping halide has on the overall three-dimensional structure. The former study has demonstrated that the capping chloride anion can act as a bridging or terminal ligand and plays a significant role in how the metal centers are connected to one another.<sup>17</sup> The latter study has resulted in only terminal halide species but, as bromine and iodine are larger than chlorine, have resulted in more open three-dimensional frameworks as a result of the size of the halides as well as possess a differing connectivity of the layers.<sup>18</sup> Thus it appeared to us that

functionalizing the capping group may provide a means to create more structural diversity in the borate system. As such, perchlorate was chosen because it is a monovalent oxoanion as well as for its inner/outer-sphere ability, variation in bonding modes, and size.

## EXPERIMENTAL SECTION

**Syntheses. Caution!** Perchlorates are known to be highly reactive when combined with organics and known to decompose under shock. Heating to over 270 °C allows for the potential release of oxygen and thus reactions with perchlorate must be monitored very carefully.

All reactants were of reagent grade and used as received without any further purification: LnCl<sub>3</sub>·6H<sub>2</sub>O (Alfa Aesar 99.99%), H<sub>3</sub>BO<sub>3</sub> (Alfa Aesar 99.5% min, ACS), and HClO<sub>4</sub> (Sigma Aldrich 70%, ACS). LnCl<sub>3</sub>·6H<sub>2</sub>O (100 mg; 0.273–0.283 mmol) (Ln = La–Nd, Sm, Eu) was charged into a poly(tetrafluoroethylene) (PTFE)-lined Parr 4749 autoclave with a 23 mL internal volume and dissolved using 300  $\mu$ L of concentrated (11 M) perchloric acid. Boric acid (422–437 mg; 6.82–

7.07 mmol) was added to the solution and the autoclave sealed. The samples were heated at 240 °C for either three, five, or seven days under autogenous pressure followed by cooling to room temperature at a rate of 3 °C per hour. The resulting materials were washed extensively with boiling deionized water to remove any excess reactants. Washing was always necessary as the products were contained in a solid mass of recrystallized boric acid and, as such, these reactions did not result in pure phases. While the bulk samples were of the appropriate color for the respective lanthanide (i.e., green for Pr, purple for Nd, and pale yellow for Sm), all resulting crystals appeared to be colorless tablets that had the propensity to stack on top of one another.

**Crystallographic Studies.** Crystals of all compounds were mounted on CryoLoops with Krytox oil and optically aligned on a Bruker APEXII Quazar X-ray diffractometer using a digital camera. Initial intensity measurements were performed using an  $I\mu S$  X-ray source, a 30 W microfocused sealed tube (Mo  $K\alpha$ ,  $\lambda = 0.71073$  Å) with high-brilliance and high-performance focusing Quazar multilayer optics. Standard APEXII software was used for determination of the unit cells and data collection control. The intensities of reflections of a sphere were collected by a combination of four sets of exposures (frames). Each set had a different  $\varphi$  angle for the crystal and each exposure covered a range of 0.5° in  $\omega$ . A total of 1464 frames were collected with an exposure time per frame of 10 to 50 s, depending on the crystal. SAINT software was used for data integration including Lorentz and polarization corrections. Semiempirical absorption corrections were applied using the program SCALE (SADABS).<sup>19</sup> Selected crystallographic information is listed in Tables 1 and 2. Atomic coordinates and additional structural information are provided in the Supporting Information (CIFs).

It should be noted that for  $\text{Ln}[\text{B}_8\text{O}_{10}(\text{OH})_6(\text{H}_2\text{O})(\text{ClO}_4)] \cdot 0.5\text{H}_2\text{O}$  the reported and calculated  $Z$  values differ. We have used a  $Z$ -value of four instead of two for the formula because the latter implies that there are two crystallographically unique metal centers when, in fact, there are not. Also, the hydrogen atoms were not found from the difference map, but assignments of protonated oxygens were determined from bond valence sum calculations<sup>20</sup> (Supporting Information Tables 3–6) for bound hydroxides and bound waters. Crystallographic information coupled with energy-dispersive spectroscopy analysis, which gave no indication of any other metal cations present, allows for the assignment of the unbound water molecule in the interlayer spaces.

**Energy-Dispersive Spectroscopy (EDS).** Energy-dispersive spectroscopy (EDS) data were collected using a LEO model EVO 50 system with an Oxford INCA energy-dispersive spectrometer. The energy of the electron beam was 20.00 kV, and the spectrum acquisition time was 120 s. All of the data were calibrated with standards, and all EDS results are provided in the Supporting Information (Figures SI 1–11). Chlorine was found in all phases.

**Infrared Spectroscopy.** Infrared spectra were obtained from single crystals using a SensIR technology IlluminatIR FT-IR microspectrometer. Single crystals were placed on quartz IR slides, and the spectrum was collected with a diamond ATR objective. Each spectrum was acquired from 650 to 4000  $\text{cm}^{-1}$  with a beam aperture of 100  $\mu\text{m}$ . Infrared spectra are shown in the Supporting Information (Figures SI 12–21).

## RESULTS AND DISCUSSION

When reacted with concentrated (11 M) perchloric acid ( $\text{HClO}_4$ ) and boric acid ( $\text{H}_3\text{BO}_3$ ), the early lanthanide chlorides (La–Nd, Sm, Eu) result in the formation of four different products depending on the identity of the lanthanide metal and the reaction time (i.e., three, five, or seven days). A graphical representation of the products formed as a function of reaction time is shown in Figure 1.

**Structure and Topology Description.**  $\text{Ln}[\text{B}_8\text{O}_{10}(\text{OH})_6(\text{H}_2\text{O})(\text{ClO}_4)] \cdot 0.5\text{H}_2\text{O}$ . When allowed to react with both boric and perchloric acid for three days at 240 °C, the

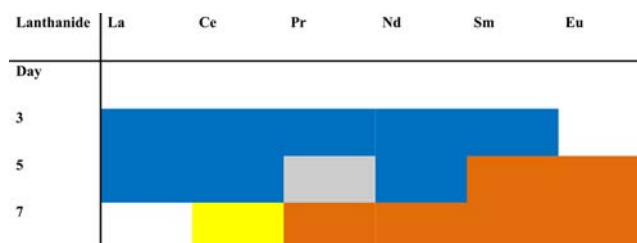


**Figure 1.** Graphical representation of the species formed as a function of both the lanthanide and the reaction time. Blue represents  $\text{Ln}[\text{B}_8\text{O}_{10}(\text{OH})_6(\text{H}_2\text{O})(\text{ClO}_4)] \cdot 0.5\text{H}_2\text{O}$  ( $\text{Ln} = \text{La}–\text{Sm}$ ), gray represents  $\text{Pr}[\text{B}_8\text{O}_{10}(\text{OH})_4(\text{H}_2\text{O})(\text{ClO}_4)]$ , orange represents  $\text{Ln}[\text{B}_7\text{O}_{11}(\text{OH})(\text{H}_2\text{O})_2(\text{ClO}_4)]$  ( $\text{Ln} = \text{Pr}–\text{Eu}$ ), and yellow represents  $\text{Ce}[\text{B}_8\text{O}_{11}(\text{OH})_4(\text{H}_2\text{O})(\text{ClO}_4)]$ .

lanthanide chlorides ( $\text{Ln} = \text{La}–\text{Nd}, \text{Sm}$ ) result in the formation of  $\text{Ln}[\text{B}_8\text{O}_{10}(\text{OH})_6(\text{H}_2\text{O})(\text{ClO}_4)] \cdot 0.5\text{H}_2\text{O}$ .  $\text{Ln}[\text{B}_8\text{O}_{10}(\text{OH})_6(\text{H}_2\text{O})(\text{ClO}_4)] \cdot 0.5\text{H}_2\text{O}$  crystallizes in the centrosymmetric, monoclinic space group  $P2_1/n$  and is a two-dimensional, layered structure (Figure 2a) which extends in the  $[bc]$  plane and is composed of sheets extending in the  $[ab]$  plane (Figure 2b). The sheets are made of corner sharing  $\text{BO}_3$  and  $\text{BO}_4$  units that create triangular holes in which the lanthanide centers reside. Each triangular hole is composed of two  $\text{BO}_3$  units and one  $\text{BO}_4$  unit which edge-share to provide six nearly coplanar oxygen atoms to the metal centers. Within the sheet, a  $\mu_3$ -oxo atom can be found in clusters formed by three corner-sharing  $\text{BO}_4$  tetrahedra. It is this cluster, along with the  $\text{BO}_3$  and  $\text{BO}_4$  units that create the triangular holes, that binds one metal center to another within the sheet.

As the borate network provides six nearly coplanar oxygen atoms in the equatorial plane of the metal center, an unusual ten-coordinate geometry, best described as a capped triangular cupola,<sup>21</sup> is observed (Figure 3a). The three base sites consist of oxygen atoms from two corner-shared  $\text{BO}_3$  units (O5 and O9) and one water moiety (O17). The capping site is occupied by a terminal, monodentate perchlorate moiety (O4). Both the base and the capping units extend into the interlayer space which is also residence for a cocrystallized water.

The bond lengths observed in these compounds are typical of what has been reported for the lanthanide borates.<sup>17,18,22–24</sup> The equatorial bond lengths range from 2.541(4) to 2.745(5) Å while the capping oxygen distances range from 2.405(5) to 2.510(4) Å for  $\text{La}[\text{B}_8\text{O}_{10}(\text{OH})_6(\text{H}_2\text{O})(\text{ClO}_4)] \cdot 0.5\text{H}_2\text{O}$  (**LaBCIO-1**),  $\text{Ce}[\text{B}_8\text{O}_{10}(\text{OH})_6(\text{H}_2\text{O})(\text{ClO}_4)] \cdot 0.5\text{H}_2\text{O}$  (**CeBCIO-1**),  $\text{Pr}[\text{B}_8\text{O}_{10}(\text{OH})_6(\text{H}_2\text{O})(\text{ClO}_4)] \cdot 0.5\text{H}_2\text{O}$  (**PrBCIO-1**),  $\text{Nd}[\text{B}_8\text{O}_{10}(\text{OH})_6(\text{H}_2\text{O})(\text{ClO}_4)] \cdot 0.5\text{H}_2\text{O}$  (**NdBCIO-1**), and  $\text{Sm}[\text{B}_8\text{O}_{10}(\text{OH})_6(\text{H}_2\text{O})(\text{ClO}_4)] \cdot 0.5\text{H}_2\text{O}$  (**SmBCIO-1**). The metal–oxygen base bond lengths range from 2.493(5) to 2.613(4) Å while the oxygen of the base water moiety range in distance from 2.335(6) to 2.429(4) Å for **LaBCIO-1**, **CeBCIO-1**, **PrBCIO-1**, **NdBCIO-1**, and **SmBCIO-1**. Individual bond lengths can be found in Table 3. The perchlorate bond distances and angles (Supporting Information Table 1) are consistent with what has previously been reported.<sup>8</sup>

$\text{Pr}[\text{B}_8\text{O}_{11}(\text{OH})_4(\text{H}_2\text{O})(\text{ClO}_4)]$ . When allowed to react with both boric and perchloric acid for five days at 240 °C,  $\text{PrCl}_3 \cdot 6\text{H}_2\text{O}$  results in the formation of  $\text{Pr}[\text{B}_8\text{O}_{11}(\text{OH})_4(\text{H}_2\text{O})(\text{ClO}_4)]$  (**PrBCIO-2**). **PrBCIO-2** crystallizes in the centrosymmetric, monoclinic space group  $P2_1/c$  and is now a three-dimensional framework structure (Figure 4a) that extends in the  $[bc]$  plane and is composed of sheets, identical to that of

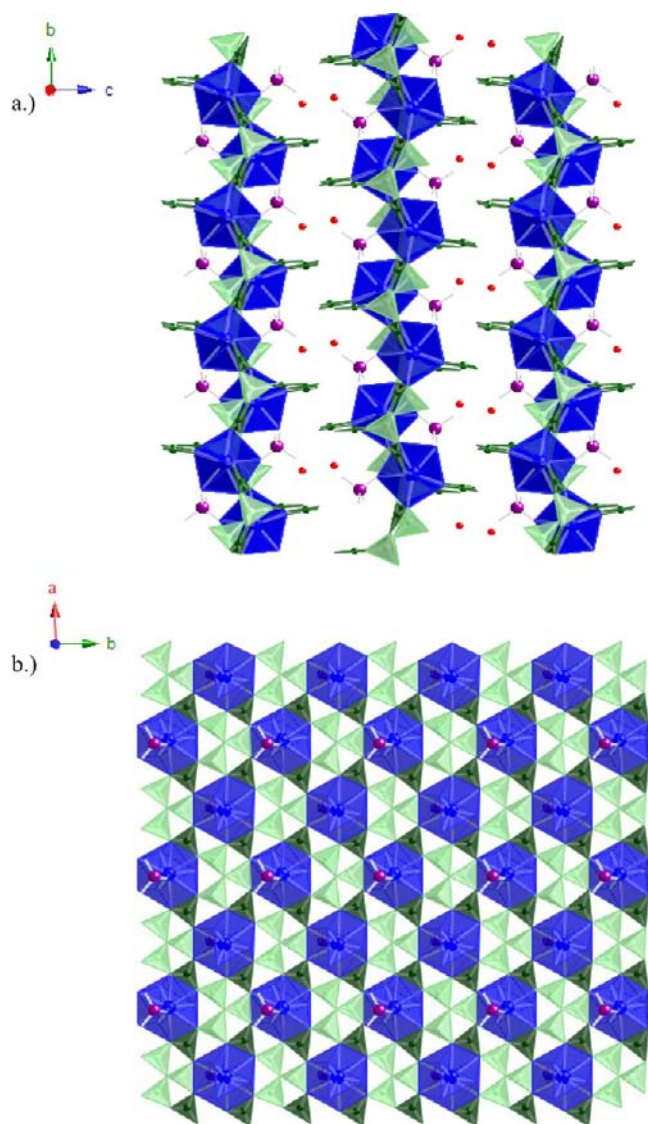


**Figure 2.** Depiction of the (a) two-dimensional sheet structure and (b) sheet topology of  $\text{Ln}[\text{B}_8\text{O}_{10}(\text{OH})_6(\text{H}_2\text{O})(\text{ClO}_4)] \cdot 0.5\text{H}_2\text{O}$  ( $\text{Ln} = \text{La}–\text{Sm}$ ). The lanthanide metal centers are depicted by the blue spheres, chlorine by purple spheres,  $\text{BO}_4$  tetrahedra by light green units,  $\text{BO}_3$  triangles as dark green units, and the water moiety as red spheres.

$\text{Ln}[\text{B}_8\text{O}_{10}(\text{OH})_6(\text{H}_2\text{O})(\text{ClO}_4)] \cdot 0.5\text{H}_2\text{O}$  ( $\text{Ln} = \text{La}–\text{Nd}, \text{Sm}$ ), which extend in the  $[ab]$  plane (Figure 2b). The praseodymium metal center exhibits a ten-coordinate, capped triangular cupola geometry (Figure 3b). This geometry is obtained as a result of the same factors discussed above. However, the three base sites are composed of oxygens from a water moiety (O18) and two corner shared  $\text{BO}_3$  units while the capping site is from a perchlorate oxygen (O4).

The layers are tethered together by the two “end-to-end”  $\text{BO}_3$  units bound to the base sites of the metal centers and by one  $\text{BO}_4$  unit from the  $\mu_3$  oxo-unit observed in the sheets. This mode of tethering the layers together creates a rather large void space in which the perchlorate moieties reside. The bond lengths observed in **PrBClO-2** are very similar to that of the **LnBClO-1** species even though the structures are different. The equatorial bond lengths range from 2.527(6) to 2.629(6) Å with the capping oxygen distance at 2.478(7) Å. The metal–oxygen base bond lengths are 2.437(8) and 2.572(8) Å with the

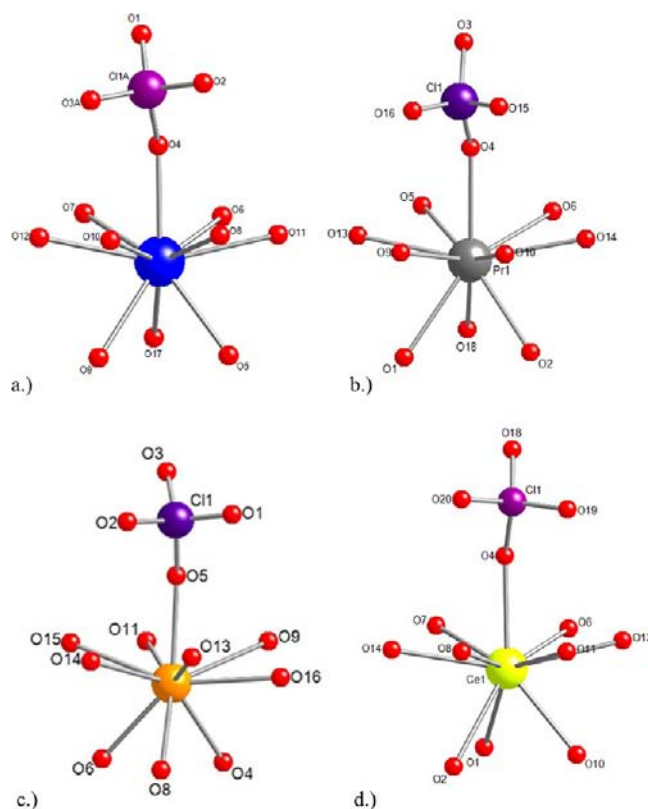


**Figure 3.** Coordination geometries and labeled bonds in (a)  $\text{Ln}[\text{B}_8\text{O}_{10}(\text{OH})_6(\text{H}_2\text{O})(\text{ClO}_4)] \cdot 0.5\text{H}_2\text{O}$  ( $\text{Ln} = \text{La}–\text{Sm}$ ), (b)  $\text{Ln}[\text{B}_7\text{O}_{11}(\text{OH})(\text{H}_2\text{O})_2(\text{ClO}_4)]$  ( $\text{Ln} = \text{Pr}–\text{Eu}$ ), (c)  $\text{Pr}[\text{B}_8\text{O}_{11}(\text{OH})_4(\text{H}_2\text{O})(\text{ClO}_4)]$ , and (d)  $\text{Ce}[\text{B}_8\text{O}_{11}(\text{OH})_4(\text{H}_2\text{O})(\text{ClO}_4)]$ . The lanthanide metal centers are depicted by blue, orange, gray, or yellow sphere, oxygens as red spheres, and chlorine as purple spheres.

oxygen of the water moiety at a distance of 2.475(9) Å (Table 4). The perchlorate bond distances and angles (Supporting Information Table 2) are consistent with what has previously been reported.<sup>8</sup>

$\text{Ln}[\text{B}_7\text{O}_{11}(\text{OH})(\text{H}_2\text{O})_2(\text{ClO}_4)]$ . When allowed to react with both boric and perchloric acid for five or seven days at 240 °C, praseodymium through europium chloride results in  $\text{Ln}[\text{B}_7\text{O}_{11}(\text{OH})(\text{H}_2\text{O})_2(\text{ClO}_4)]$  ( $\text{Ln} = \text{Pr}, \text{Nd}, \text{Sm}, \text{Eu}$ ) for five (**SmBClO-2** and **EuBClO-1**) and seven days (**PrBClO-3**, **NdBClO-2**, **SmBClO-2**, and **EuBClO-1**).  $\text{Ln}[\text{B}_7\text{O}_{11}(\text{OH})(\text{H}_2\text{O})_2(\text{ClO}_4)]$  crystallizes in the centrosymmetric, monoclinic space group  $P2_1/n$  and is a three-dimensional framework structure (Figure 4b) which extends in the  $[ab]$  plane. The three-dimensional network is composed of sheets, identical to that of all other compounds presented in this work, which extend in the  $[ac]$  plane (Figure 2b) but, again, differ by how they are linked together. The metal centers exhibit a ten-coordinate, capped triangular cupola geometry (Figure 3c). The three base sites are now composed of oxygens from two water moieties (O4 and O6) and one  $\text{BO}_3$  unit (O8) with the capping site from a perchlorate oxygen (O5).

The layers are tethered together by the  $\text{BO}_3$  unit bound to the base sites of the metal centers and by one  $\text{BO}_4$  unit of the  $\mu_3$  oxo-unit observed in the sheet topology. Furthermore, while two “end-to-end”  $\text{BO}_3$  units are required to bind the layers together, the arrangement of these units is different than what is observed in **PrBClO-2**. It can be seen that one  $\text{BO}_3$  triangle is

**Table 3. Selected Bond Distances (Å) for La[B<sub>8</sub>O<sub>10</sub>(OH)<sub>6</sub>(H<sub>2</sub>O)(ClO<sub>4</sub>)]·0.5H<sub>2</sub>O (LaBClO-1), Ce[B<sub>8</sub>O<sub>10</sub>(OH)<sub>6</sub>(H<sub>2</sub>O)(ClO<sub>4</sub>)]·0.5H<sub>2</sub>O (CeBClO-1), Pr[B<sub>8</sub>O<sub>10</sub>(OH)<sub>6</sub>(H<sub>2</sub>O)(ClO<sub>4</sub>)]·0.5H<sub>2</sub>O (PrBClO-1), Nd[B<sub>8</sub>O<sub>10</sub>(OH)<sub>6</sub>(H<sub>2</sub>O)(ClO<sub>4</sub>)]·0.5H<sub>2</sub>O (NdBClO-1), Sm[B<sub>8</sub>O<sub>10</sub>(OH)<sub>6</sub>(H<sub>2</sub>O)(ClO<sub>4</sub>)]·0.5H<sub>2</sub>O (SmBClO-1)**

distance (Å)				distance (Å)			
equatorial		base		equatorial		base	
La(1)–O(4)	2.510(4)	La(1)–O(5)	2.613(4)	Nd(1)–O(4)	2.438(4)	Nd(1)–O(5)	2.563(4)
La(1)–O(6)	2.707(4)	La(1)–O(9)	2.573(4)	Nd(1)–O(6)	2.693(4)	Nd(1)–O(9)	2.513(4)
La(1)–O(7)	2.712(4)	La(1)–O(17)	2.429(4)	Nd(1)–O(7)	2.713(4)	Nd(1)–O(17)	2.365(4)
La(1)–O(8)	2.658(4)			Nd(1)–O(8)	2.620(4)		
La(1)–O(10)	2.675(4)			Nd(1)–O(10)	2.627(4)		
La(1)–O(11)	2.591(4)			Nd(1)–O(11)	2.557(4)		
La(1)–O(12)	2.587(4)			Nd(1)–O(12)	2.562(4)		
Ce(1)–O(4)	2.473(3)	Ce(1)–O(5)	2.609(3)	Sm(1)–O(4)	2.405(5)	Sm(1)–O(5)	2.541(5)
Ce(1)–O(6)	2.709(2)	Ce(1)–O(9)	2.555(3)	Sm(1)–O(6)	2.728(4)	Sm(1)–O(9)	2.493(5)
Ce(1)–O(7)	2.723(2)	Ce(1)–O(17)	2.400(3)	Sm(1)–O(7)	2.745(4)	Sm(1)–O(17)	2.335(5)
Ce(1)–O(8)	2.635(2)			Sm(1)–O(8)	2.602(4)		
Ce(1)–O(10)	2.646(2)			Sm(1)–O(10)	2.609(4)		
Ce(1)–O(11)	2.577(2)			Sm(1)–O(11)	2.541(4)		
Ce(1)–O(12)	2.578(2)			Sm(1)–O(12)	2.550(4)		
Pr(1)–O(4)	2.449(5)	Pr(1)–O(5)	2.566(5)				
Pr(1)–O(6)	2.704(5)	Pr(1)–O(9)	2.526(5)				
Pr(1)–O(7)	2.717(5)	Pr(1)–O(17)	2.372(6)				
Pr(1)–O(8)	2.626(5)						
Pr(1)–O(10)	2.622(5)						
Pr(1)–O(11)	2.561(5)						
Pr(1)–O(12)	2.562(5)						

twisted and bound perpendicular to the other BO<sub>3</sub> triangle found in the “end-to-end” attachment (Figure 4b). This mode of tethering creates a smaller, more compacted void space in which the perchlorate moieties reside and, therefore, results in a more dense structure (Table 2). The bond lengths are similar to that of the other species discussed in this work. The equatorial bond lengths range from 2.515(5) to 2.734(7) Å with the capping oxygen distance ranging from 2.390(5) to 2.460(8) Å for PrBClO-3, NdBClO-2, SmBClO-2, and EuBClO-1. The base water bond lengths range from 2.432(5) to 2.488(6) Å while the oxygen distances of the BO<sub>3</sub> moiety range from 2.490(5) to 2.572(8) Å for PrBClO-3, NdBClO-2, SmBClO-2, and EuBClO-1. Individual bond lengths can be found in Table 4. The perchlorate bond distances and angles (Supporting Information Table 2) are consistent with what has previously been reported.<sup>8</sup>

*Ce[B<sub>8</sub>O<sub>11</sub>(OH)<sub>4</sub>(H<sub>2</sub>O)(ClO<sub>4</sub>)].* When allowed to react with both boric and perchloric acid for seven days at 240 °C, CeCl<sub>3</sub>·6H<sub>2</sub>O results in the formation of Ce-[B<sub>8</sub>O<sub>11</sub>(OH)<sub>4</sub>(H<sub>2</sub>O)(ClO<sub>4</sub>)] (CeBClO-2). CeBClO-2 crystallizes in the centrosymmetric, monoclinic space group *P*2<sub>1</sub>/*n* and is a three-dimensional framework structure (Figure 4c) which extends in the [*ab*] plane. The three-dimensional network is composed of sheets, identical to that of all other compounds presented in this work, which extends in the [*ac*] plane (Figure 2b). The metal centers exhibit a ten-coordinate, capped triangular cupola geometry (Figure 3d). The three base sites are composed of oxygens from one water moiety (O1) and two corner sharing BO<sub>3</sub> units (O2 and O10) with the capping site provided by a perchlorate oxygen (O4).

The layers are tethered together by the two BO<sub>3</sub> units bound to the base sites of the metal centers and by one BO<sub>4</sub> unit from the μ<sub>3</sub> oxo-unit observed in the sheet topology. The equatorial

bond lengths range from 2.552(7) to 2.656(7) Å with the capping oxygen (O4) distance at 2.481(8) Å. The base bond lengths are 2.452(8) and 2.606(8) Å (O2 and O10) with the oxygen of the water moiety (O1) at a distance of 2.506(9) Å (Table 4). The perchlorate bond distances and angles (Supporting Information Table 2) are consistent with what has previously been reported.<sup>8</sup>

*Infrared Spectroscopy.* The free perchlorate anion (ClO<sub>4</sub><sup>−</sup>) is a tetrahedron and possesses *T<sub>d</sub>* symmetry. As such, four fundamental vibrations would be present, two of which are strictly Raman active vibrations. The remaining IR active vibrations are the asymmetric stretching mode around 1115 cm<sup>−1</sup> and asymmetric bending mode around 630 cm<sup>−1</sup>.<sup>25</sup> Of course, perchlorate bound in a structure would result in a deviation from a perfect tetrahedron and as such the vibrational energy of each mode will be shifted slightly. Borate vibrational bands are generally assigned between 1400–1100 cm<sup>−1</sup> and 1000–800 cm<sup>−1</sup> for BO<sub>3</sub> and BO<sub>4</sub>, respectively.<sup>26,27</sup>

The IR spectrum for LaBClO-1 can be seen in Figure 5 while the remaining spectra can be seen in Supporting Information, Figures 12–21. The antisymmetric stretches around 1250 cm<sup>−1</sup> and 1363 cm<sup>−1</sup> are consistent with the existence of a BO<sub>3</sub> unit while the bands near 920 cm<sup>−1</sup> are consistent with that of a BO<sub>4</sub> unit. The vibrational band around 1150 cm<sup>−1</sup> can be assigned to the asymmetric stretching mode of perchlorate (Figure 5). The IR spectrum also shows the presence of both the bound water –OH vibration and free, cocrystallized water –OH vibration (Figure 5).

*Periodic Trends.* The trivalent lanthanides represent a unique series where fine control of the ionic radius is easily obtained, as the lanthanide contraction is relatively constant as the series is traversed. While examples are known, lanthanide complexes with coordination number ten are atypical when

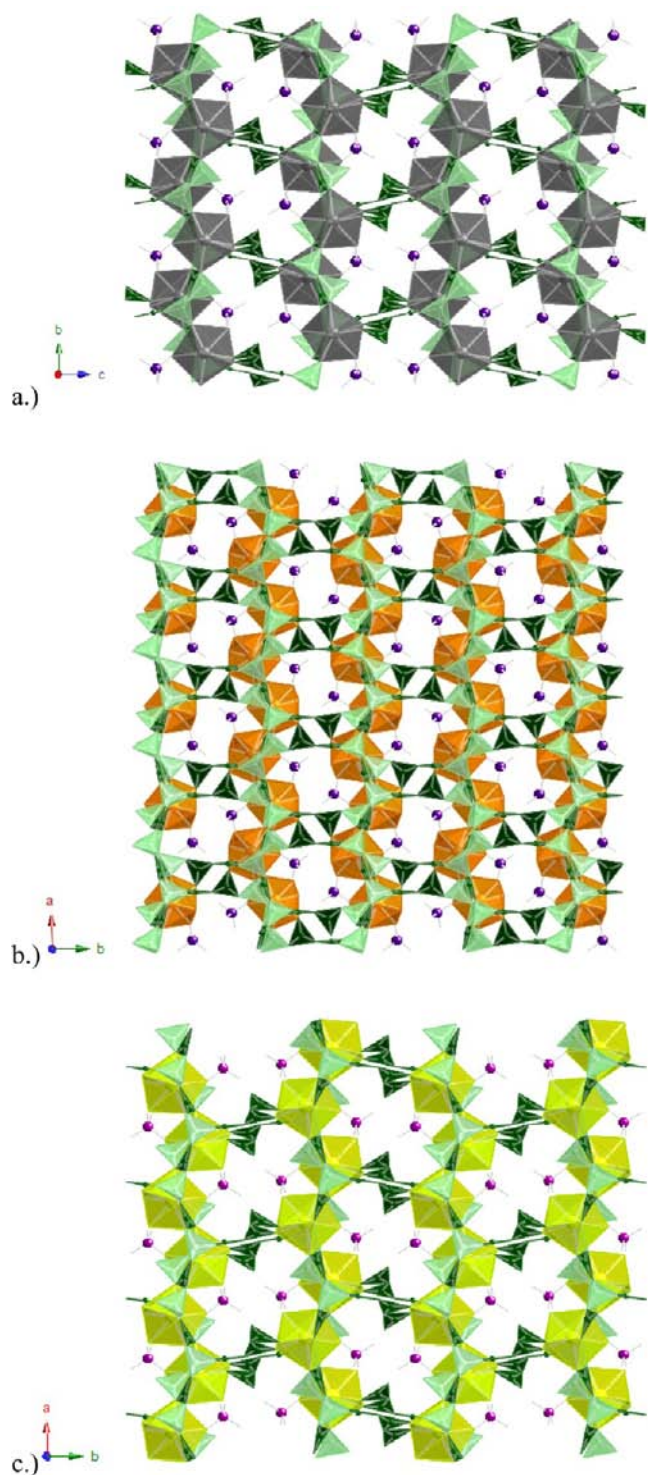


**Figure 4.** Three dimensional framework structure of (a)  $\text{Pr}[\text{B}_8\text{O}_{11}(\text{OH})_4(\text{H}_2\text{O})(\text{ClO}_4)]$ , (b)  $\text{Ln}[\text{B}_7\text{O}_{11}(\text{OH})(\text{H}_2\text{O})_2(\text{ClO}_4)]$  ( $\text{Ln} = \text{Pr-Eu}$ ), and (c)  $\text{Ce}[\text{B}_8\text{O}_{11}(\text{OH})_4(\text{H}_2\text{O})(\text{ClO}_4)]$ . The lanthanide metal center is depicted as gray, orange, or yellow spheres, chlorine by purple spheres,  $\text{BO}_4$  tetrahedra by light green units, and  $\text{BO}_3$  triangles as dark green units.

compared with coordination numbers of eight or nine.<sup>21,28</sup> The most typical geometries for ten-coordinate complexes are the bicapped square antiprism and sphenocorona, while less common geometries are known.<sup>21</sup>

Referring back to Figure 1, with a reaction time of only three days, the lanthanides chlorides ( $\text{La-Nd}$ ,  $\text{Sm}$ ) result in the formation of  $\text{Ln}[\text{B}_8\text{O}_{10}(\text{OH})_6(\text{H}_2\text{O})(\text{ClO}_4)] \cdot 0.5\text{H}_2\text{O}$  which is a two-dimensional layered structure. It should be noted that no product was obtained for the three day reaction when europium trichloride was present. When the reaction time is increased to five days, a slightly different picture emerges resulting in three products:  $\text{Ln}[\text{B}_8\text{O}_{10}(\text{OH})_6(\text{H}_2\text{O})(\text{ClO}_4)] \cdot 0.5\text{H}_2\text{O}$  ( $\text{Ln} = \text{La}$ ,  $\text{Ce}$ ,  $\text{Nd}$ ) (**LaBClO-1**, **CeBClO-1**, and **NdBClO-1**),  $\text{Pr}[\text{B}_8\text{O}_{11}(\text{OH})_4(\text{H}_2\text{O})(\text{ClO}_4)]$  (**PrBClO-2**), and  $\text{Ln}[\text{B}_7\text{O}_{11}(\text{OH})(\text{H}_2\text{O})_2(\text{ClO}_4)]$  ( $\text{Ln} = \text{Sm}$ ,  $\text{Eu}$ ) (**SmBClO-2** and **EuBClO-1**). On the basis of size, it would be expected that under these conditions praseodymium would also form the  $\text{Ln}[\text{B}_8\text{O}_{10}(\text{OH})_6(\text{H}_2\text{O})(\text{ClO}_4)] \cdot 0.5\text{H}_2\text{O}$  structure. Deviation from this expectation suggests that the **PrBClO-2** structure resides in a kinetic well. It is less surprising that a structural change occurs between **NdBClO-1** and **SmBClO-2** as the highly radioactive promethium separates these lanthanide metals and, as such, a larger change in ionic radii follows.<sup>29</sup>

When reacted for seven days, the final outcome of this system appears with the formation of two products:  $\text{Ln}[\text{B}_7\text{O}_{11}(\text{OH})(\text{H}_2\text{O})_2(\text{ClO}_4)]$  ( $\text{Ln} = \text{Pr}$ ,  $\text{Nd}$ ,  $\text{Sm}$ ,  $\text{Eu}$ ) (**PrBClO-3**, **NdBClO-2**, **SmBClO-2**, **EuBClO-1**) and  $\text{Ce}[\text{B}_8\text{O}_{11}(\text{OH})_4(\text{H}_2\text{O})(\text{ClO}_4)]$  (**CeBClO-2**).  $\text{Ce}[\text{B}_8\text{O}_{11}(\text{OH})_4(\text{H}_2\text{O})(\text{ClO}_4)]$  (**CeBClO-2**) is the outcast of this reaction scheme as it forms a product with the same formula as **PrBClO-2**. While the chemical formulas may be the same, **CeBClO-2** and **PrBClO-2** crystallize in different space groups, have different lattice parameters, and **CeBClO-2** possesses pseudo-orthorhombic symmetry. The lanthanum product poorly crystallizes, even with several attempts, and appears to form the **CeBClO-2** product. The seven day reaction products are also obtained with heating times of up to ten days. As no changes in products or additional products were observed in going from seven to ten days, no further reaction times were investigated.

All of the compounds presented in this work have the same sheet topology (Figure 2b), and all metal centers are ten-coordinate with the capped triangular cupola geometry (Figure 3). This geometry is obtained as the borate network provides six nearly coplanar oxygen atoms (four oxygen atoms from two  $\text{BO}_3$  units and two oxygen atoms from one  $\text{BO}_4$  unit) which create the triangular holes in which the metal centers reside. All metal centers also contain only  $\text{BO}_3$  or water units attached on the base sites and a terminal, monodentate perchlorate moiety in the capping position. What differentiates these structures is the way the  $\text{BO}_3$  units of the metal base sites are used to tether (or not tether) the layers together.

It is interesting to note that in all compounds in this work, the coordination number remains at ten while in our previous work using the same lanthanides and without perchlorate present, a transition from ten-coordinate to nine-coordinate occurs between neodymium and samarium for  $\text{Nd}[\text{B}_4\text{O}_6(\text{OH})_2\text{Cl}]$  and  $\text{Sm}_4[\text{B}_{18}\text{O}_{25}(\text{OH})_{13}\text{Cl}_3]$  and praseodymium and neodymium for  $\text{Pr}[\text{B}_5\text{O}_8(\text{OH})(\text{H}_2\text{O})_2\text{Br}]$  and  $\text{Nd}_4[\text{B}_{18}\text{O}_{25}(\text{OH})_{13}\text{Br}_3]$ .<sup>17,18,30</sup> However, like what is presented here, when the large iodine atom is present in the structure, no change in coordination number is observed.<sup>18</sup> Furthermore, our previously reported lanthanide borate chlorides were more likely to have  $\text{BO}_4$  units bound to the base sites whereas the species in this work contain exclusively  $\text{BO}_3$  and water moieties.<sup>17</sup>

**Table 4.** Selected Bond Distances (Å) for Ce[B<sub>8</sub>O<sub>11</sub>(OH)<sub>4</sub>(H<sub>2</sub>O)(ClO<sub>4</sub>)] (CeBClO-2), Pr[B<sub>8</sub>O<sub>11</sub>(OH)<sub>4</sub>(H<sub>2</sub>O)(ClO<sub>4</sub>)] (PrBClO-2), Pr[B<sub>7</sub>O<sub>11</sub>(OH)(H<sub>2</sub>O)<sub>2</sub>(ClO<sub>4</sub>)] (PrBClO-3), Nd[B<sub>7</sub>O<sub>11</sub>(OH)(H<sub>2</sub>O)<sub>2</sub>(ClO<sub>4</sub>)] (NdBClO-2), Sm[B<sub>7</sub>O<sub>11</sub>(OH)(H<sub>2</sub>O)<sub>2</sub>(ClO<sub>4</sub>)] (SmBClO-2), and Eu[B<sub>7</sub>O<sub>11</sub>(OH)(H<sub>2</sub>O)<sub>2</sub>(ClO<sub>4</sub>)] (EuBClO-1)

distance (Å)				distance (Å)			
equatorial		base		equatorial		base	
Ce(1)–O(4)	2.481(8)	Ce(1)–O(1)	2.506(9)	Nd(1)–O(5)	2.439(5)	Nd(1)–O(4)	2.476(5)
Ce(1)–O(6)	2.655(7)	Ce(1)–O(2)	2.606(8)	Nd(1)–O(9)	2.720(5)	Nd(1)–O(6)	2.483(5)
Ce(1)–O(7)	2.623(7)	Ce(1)–O(10)	2.452(8)	Nd(1)–O(11)	2.590(5)	Nd(1)–O(8)	2.547(5)
Ce(1)–O(8)	2.600(7)			Nd(1)–O(13)	2.550(5)		
Ce(1)–O(11)	2.656(7)			Nd(1)–O(14)	2.662(5)		
Ce(1)–O(13)	2.618(7)			Nd(1)–O(15)	2.563(5)		
Ce(1)–O(14)	2.552(7)			Nd(1)–O(16)	2.548(5)		
Pr(1)–O(4)	2.478(7)	Pr(1)–O(1)	2.572(8)	Sm(1)–O(5)	2.404(4)	Sm(1)–O(4)	2.450(3)
Pr(1)–O(5)	2.629(6)	Pr(1)–O(2)	2.437(8)	Sm(1)–O(9)	2.720(3)	Sm(1)–O(6)	2.458(3)
Pr(1)–O(6)	2.626(6)	Pr(1)–O(18)	2.475(9)	Sm(1)–O(11)	2.575(3)	Sm(1)–O(8)	2.521(3)
Pr(1)–O(9)	2.614(6)			Sm(1)–O(13)	2.531(3)		
Pr(1)–O(10)	2.629(6)			Sm(1)–O(14)	2.639(3)		
Pr(1)–O(13)	2.527(6)			Sm(1)–O(15)	2.555(3)		
Pr(1)–O(14)	2.596(6)			Sm(1)–O(16)	2.525(3)		
Pr(1)–O(5)	2.460(8)	Pr(1)–O(4)	2.484(7)	Eu(1)–O(5)	2.390(5)	Eu(1)–O(4)	2.432(5)
Pr(1)–O(9)	2.734(7)	Pr(1)–O(6)	2.488(8)	Eu(1)–O(9)	2.696(4)	Eu(1)–O(6)	2.441(5)
Pr(1)–O(11)	2.605(7)	Pr(1)–O(8)	2.572(8)	Eu(1)–O(11)	2.559(5)	Eu(1)–O(8)	2.490(5)
Pr(1)–O(13)	2.567(7)			Eu(1)–O(13)	2.515(5)		
Pr(1)–O(14)	2.671(7)			Eu(1)–O(14)	2.622(5)		
Pr(1)–O(15)	2.574(7)			Eu(1)–O(15)	2.530(5)		
Pr(1)–O(16)	2.559(7)			Eu(1)–O(16)	2.517(5)		

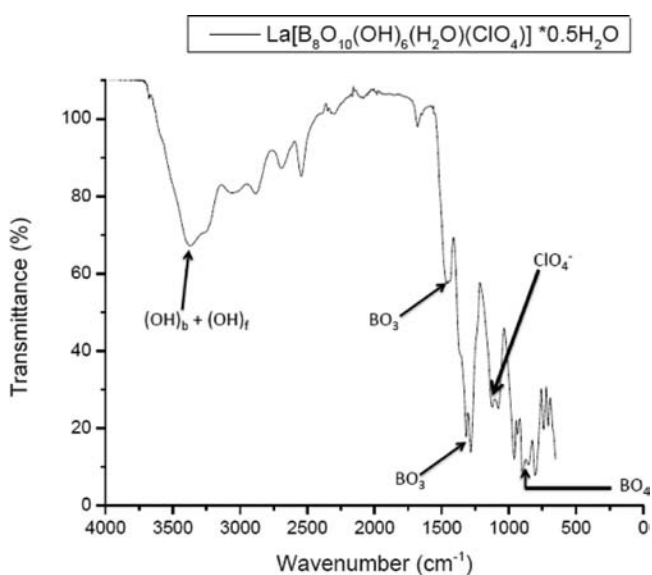


**Figure 5.** IR spectrum of La[B<sub>8</sub>O<sub>10</sub>(OH)<sub>6</sub>(H<sub>2</sub>O)(ClO<sub>4</sub>)]·0.5H<sub>2</sub>O with the stretching modes of hydroxide, perchlorate, and borate units identified.

These differences are attributed to two factors. The first is the low pH used to synthesize the title lanthanide borate perchlorate species. Boric acid tends to behave as a hydroxide acceptor rather than a proton donor,<sup>26</sup> and as such, more BO<sub>3</sub> units are expected in the resulting borate species when the reaction conditions are more acidic than basic. The second factor is the large size of the perchlorate ligand. The use of a large capping ligand results in the short reaction time products (LnBClO-1; Ln = La–Nd, Sm) forming two-dimensional

layered structures. When the layers are indeed connected in the remaining structures of this work, a double, “end-to-end” tethering unit composed of two BO<sub>3</sub> triangles is required. The only other example of this “end-to-end” borate binding of layers can be found in our previously reported Pu[B<sub>7</sub>O<sub>11</sub>(OH)(H<sub>2</sub>O)<sub>2</sub>] structure which is isotopic to the Ln[B<sub>7</sub>O<sub>11</sub>(OH)(H<sub>2</sub>O)<sub>2</sub>(ClO<sub>4</sub>)] products of this work.<sup>18</sup>

## CONCLUSIONS

The products, Ln[B<sub>8</sub>O<sub>10</sub>(OH)<sub>6</sub>(H<sub>2</sub>O)(ClO<sub>4</sub>)]·0.5H<sub>2</sub>O (Ln = La–Nd, Sm), Pr[B<sub>8</sub>O<sub>11</sub>(OH)<sub>4</sub>(H<sub>2</sub>O)(ClO<sub>4</sub>)], Ce-[B<sub>8</sub>O<sub>11</sub>(OH)<sub>4</sub>(H<sub>2</sub>O)(ClO<sub>4</sub>)], and Ln[B<sub>7</sub>O<sub>11</sub>(OH)(H<sub>2</sub>O)<sub>2</sub>(ClO<sub>4</sub>)] (Ln = Pr, Nd, Sm, Eu), all exhibit a ten-coordinate capped triangular cupola geometry with the base sites being composed of either water or BO<sub>3</sub> units. These BO<sub>3</sub> units are used to tether the layers together as well as creating the void space in which the perchlorate moiety can reside. All bond lengths in these species are typical for what has been observed in other lanthanide borates, and the perchlorate bond lengths and angles are typical as well.<sup>8,17,18,22–24</sup> The decrease observed in the unit cell constants in an isotopic series is to be expected as the lanthanide contraction is observed in this system. While the BO<sub>3</sub> and BO<sub>4</sub> vibrational modes are close to that of the perchlorate modes, the perchlorate can be identified by use of IR spectroscopy. In this report, we have found that lanthanide borates can be synthesized in low pH by using concentrated (11 M) perchloric acid directly in the reaction vessel. While it has been suggested that the perchlorate anion is noncoordinating in acidic media,<sup>4,5</sup> we have found that in this system, perchlorate is indeed inner-sphere coordinating and found as a terminal, monodentate capping ligand. Finally, this work, in combination with our previous studies, demonstrated that the capping anion plays a significant role in determining

the overall structure.<sup>17,18</sup> Certain ligands, such as chloride, can be terminal or bridge to other metal centers.<sup>17,30</sup> Compounds containing bridged ligands are generally more compact and dense structures while those with terminal ligands are generally more open. The larger capping ligands require more space and, as such, create large void spaces resulting in less compacted structures.<sup>18</sup> The larger ligands may also require unique binding arrangements to tether the layers together or may be so large as to prevent an overall three-dimensional arrangement. Perchlorate is the first such ligand that we have found that can result in a two- rather than three-dimensional borate network. As it has been shown that new lanthanide borates can be prepared at very low pH, a report on using other concentrated acids is forthcoming.

## ■ ASSOCIATED CONTENT

### ● Supporting Information

All of the EDS spectra and IR spectra of all compounds presented in this work. This material is available free of charge via the Internet at <http://pubs.acs.org>.

## ■ AUTHOR INFORMATION

### Corresponding Author

\*E-mail: [talbrecl@nd.edu](mailto:talbrecl@nd.edu).

### Notes

The authors declare no competing financial interest.

## ■ ACKNOWLEDGMENTS

We are grateful for support provided by the Chemical Sciences, Geosciences, and Biosciences Division, Office of Basic Energy Sciences, Office of Science, Heavy Elements Chemistry Program, U.S. Department of Energy, under Grant DE-FG02-09ER16026. Collaborative work with our German counterparts is supported via the Helmholtz Association, Grant VH-NG-815.

## ■ REFERENCES

- (1) Borgoo, A.; Torrent-Sucarrat, M.; De Proft, F.; Geerlings, P. J. *Chem. Phys.* **2007**, *126*, 234104.
- (2) Mikheev, N. B. *Inorg. Chim. Acta* **1984**, *94*, 241–248.
- (3) (a) Glaser, J.; Johansson, G. *Acta Chem. Scand.* **1981**, *A 35*, 639. (b) Johansson, G.; Yokoyama, H. *Inorg. Chem.* **1990**, *29*, 2460. (c) Brucher, E.; Glaser, J.; Grenthe, I.; Puigdomenech, I. *Inorg. Chim. Acta* **1985**, *109*, 111.
- (4) *Gmelins Handbuch der Anorganischen Chemie*; Springer-Verlag: Berlin, Germany, 1977; Vol C5.
- (5) Semon, L.; Boehme, C.; Billard, I.; Hennig, C.; Lutzenkirchem, K.; Reich, T.; Rossberg, A.; Rossini, L.; Wipff, G. *Chem. Phys. Chem.* **2001**, *2*, 591–598.
- (6) Torapava, N.; Persson, I.; Eriksson, L.; Lundberg, D. *Inorg. Chem.* **2009**, *48*, 11712–11723.
- (7) Ma, J.; Huang, X.; Wei, R.; Zhou, L.; Lie, W. *Inorg. Chim. Acta* **2009**, *362*, 3440–3446.
- (8) Wickleder, M.; Schäfer, W. *Z. Anorg. Allg. Chem.* **1999**, *625*, 309–312.
- (9) Pascal, J. L.; Favier, F.; Cunin, F.; Fitch, A.; Vaughan, G. J. *Solid State Chem.* **1998**, *139*, 259–265.
- (10) Galdecka, E.; Galdecki, Z.; Huskowska, E.; Amirhanov, V.; Legendziewicz, J. *J. Alloys Compd.* **1997**, *257*, 182–190.
- (11) Grigor'ev, M. S.; Antipin, M. Y.; Krot, N. N.; Garnov, A. Y. *Radiochem.* **2002**, *44*, 458–462.
- (12) Takao, S.; Takao, K.; Kraus, W.; Emmerling, F.; Scheinost, A. C.; Bernhard, G.; Hennig, C. *Eur. J. Inorg. Chem.* **2009**, 4771–4775.
- (13) Burns, P. C.; Grice, J. D.; Hawthorne, F. C. *Can. Mineral.* **1995**, *33*, 1131.
- (14) Grice, J. D.; Burns, P. C.; Hawthorne, F. C. *Can. Mineral.* **1999**, *37*, 731.
- (15) Yuan, G.; Xue, D. *Acta Crystallogr.* **2007**, *B63*, 353.
- (16) (a) Wang, S.; Alekseev, E. V.; Ling, J.; Liu, G.; Depmeier, W.; Albrecht-Schmitt, T. E. *Chem. Mater.* **2010**, *22*, 2155–2163. (b) Wang, S.; Alekseev, E. V.; Stritzinger, J. T.; Depmeier, W.; Albrecht-Schmitt, T. E. *Inorg. Chem.* **2010**, *49*, 2948–2953. (c) Wang, S.; Alekseev, E. V.; Stritzinger, J. T.; Depmeier, W.; Albrecht-Schmitt, T. E. *Inorg. Chem.* **2010**, *49*, 6690–6696. (d) Wang, S.; Alekseev, E. V.; Stritzinger, J. T.; Liu, G.; Depmeier, W.; Albrecht-Schmitt, T. E. *Chem. Mater.* **2010**, *22*, 5983–5991. (e) Wang, S.; Alekseev, E. V.; Ling, J.; Skanthakumar, S.; Soderholm, L.; Depmeier, W.; Albrecht-Schmitt, T. E. *Angew. Chem., Int. Ed.* **2010**, *49*, 1263–1266. (f) Wang, S.; Villa, E. M.; Diwu, J.; Alekseev, E. V.; Depmeier, W.; Albrecht-Schmitt, T. E. *Inorg. Chem.* **2011**, *50*, 2527–2533. (g) Wang, S.; Alekseev, E. V.; Diwu, J.; Miller, H. M.; Oliver, A.; Liu, G.; Depmeier, W.; Albrecht-Schmitt, T. E. *Chem. Mater.* **2011**, *23*, 2931–2939. (h) Wang, S.; Alekseev, E. V.; Depmeier, W.; Albrecht-Schmitt, T. E. *Chem. Com.* **2010**, *46*, 3955–3957. (i) Wang, S.; Alekseev, E. V.; Miller, H. M.; Depmeier, W.; Albrecht-Schmitt, T. E. *Inorg. Chem.* **2010**, *49*, 9755–9757. (j) Wang, S.; Alekseev, E. V.; Depmeier, W.; Albrecht-Schmitt, T. E. *Inorg. Chem.* **2011**, *50*, 2079–2081. (k) Polinski, M. J.; Wang, S.; Alekseev, E. V.; Depmeier, W.; Albrecht-Schmitt, T. E. *Angew. Chem., Int. Ed.* **2011**, *50*, 8891–8894. (l) Polinski, M. J.; Wang, S.; Alekseev, E. V.; Depmeier, W.; Liu, G.; Haire, R. G.; Albrecht-Schmitt, T. E. *Angew. Chem., Int. Ed.* **2012**, *51*, 1869–1872.
- (17) Polinski, M. J.; Grant, D. J.; Wang, S.; Alekseev, E. V.; Cross, J. N.; Villa, E. M.; Depmeier, W.; Gagliardi, L.; Albrecht-Schmitt, T. E. *J. Am. Chem. Soc.* **2012**, *134*, 10682–10692.
- (18) Polinski, M. J.; Wang, S.; Cross, J. N.; Alekseev, E. V.; Depmeier, W.; Albrecht-Schmitt, T. E. *Inorg. Chem.* **2012**, *51*, 7859–7866.
- (19) Sheldrick, G. M. *SADABS 2001, Program for absorption correction using SMART CCD based on the method of Blessing*; Blessing, R. H. *Acta Crystallogr.* **1995**, *A51*, 33.
- (20) (a) Brown, I. D.; Altermatt, D. *Acta Crystallogr.* **1985**, *B41*, 244–247. (b) Brese, N. E.; O'Keeffe, M. *Acta Crystallogr.* **1991**, *B47*, 192–197. (c) Roulhac, P. L.; Palenik, G. J. *Inorg. Chem.* **2003**, *42*, 118–121.
- (21) Ruiz-Martínez, A.; Alvarez, S. *Chem.—Eur. J.* **2009**, *15*, 7470–7480.
- (22) Li, L.; Jin, X.; Li, G.; Wang, Y.; Liao, F.; Tao, G.; Lin, J. *Chem. Mater.* **2003**, *15*, 2253–2260.
- (23) Lu, P.; Wang, Y.; Lin, J.; You, L. *Chem. Commun.* **2001**, 1178–1179.
- (24) Li, L.; Lu, P.; Wang, Y.; Jin, X.; Li, G.; Wang, Y.; You, L.; Lin, J. *Chem. Mater.* **2002**, *14*, 4963–4968.
- (25) Chen, Y.; Zhang, Y.; Zhao, L. *Phys. Chem. Phys. Chem.* **2004**, *6*, 537–542.
- (26) Peak, D.; Luther, G. W.; Sparks, D. L. *Geochim. Cosmochim. Acta* **2003**, *67*, 2251–2560.
- (27) Chen, X.; Zhao, Y.; Chang, X.; Zuo, J.; Zang, H.; Xiao, W. *J. Solid State Chem.* **2006**, *179*, 3911–3918.
- (28) Ruiz-Martínez, A.; Casanova, D.; Alvarez, S. *Chem.—Eur. J.* **2008**, *14*, 1291–1303.
- (29) Shannon, R. D. *Acta Crystallogr., Sect. A* **1976**, *32*, 751–767.
- (30) Belokoneva, E. L.; Stefanovich, S.; Dimitrova, O. V.; Ivanova, A. G. *Zh. Neorg. Khim.* **2002**, *47*, 370–377.